Available online at www.sciencedirect.com
SCIENCE DIRECT
ELSEVIER
Journal of Chromatography B, 840 (2006) 1–9
JOURNAL OF CHROMATOGRAPHY B
www.elsevier.com/locate/chromb

Changes of the cortex proteome and Apolipoprotein E in transgenic mouse models of Alzheimer's Disease☆

O. Carrette[a,*], J.A. Burgess[b], P.R. Burkhard[a,c], C. Lang[d], M. Côte[a], N. Rodrigo[a,c], D.F. Hochstrasser[b,e], J.-C. Sanchez[b]

[a] *Neuroproteomics Group, Department of Structural Biology and Bioinformatics, Geneva University, Faculty of Medicine, Geneva, Switzerland*
[b] *Biomedical Proteomics Research Group, Department of Structural Biology and Bioinformatics, Geneva University, Faculty of Medicine, Geneva, Switzerland*
[c] *Neurology Department, Geneva University Hospital, Geneva, Switzerland*
[d] *Department of Econometry, Geneva University, Geneva, Switzerland*
[e] *Central Clinical Chemistry Laboratory, Geneva University Hospital, Geneva, Switzerland*

Received 9 February 2006; accepted 7 May 2006
Available online 16 June 2006

Abstract

Transgenic mice carrying human Amyloid Precursor Protein mutations present amyloid plaque deposition in the brain upon aging. In this study, we characterized the changes of cortex proteome and endogenous Apolipoprotein E in these mice. Differential analysis of two-dimensional electrophoresis images revealed spots altered upon aging, transgene addition and plaque deposition. Alpha-synuclein and cytochrome oxidase polypeptide Va were up-regulated in transgenic mice. Upon aging, expression of ATP synthase α, α enolase, UMP-CMP kinase, and dihydropyrimidinase like-2 protein was modified. These proteins and their modification probably play a role in the amyloid aggregate formation in these mice.

Keywords: Two-dimensional electrophoresis; Alzheimer's disease; Transgenic mice; Cortex

1. Introduction

A growing body of evidence suggests that abnormal processing of the Amyloid Precursor Protein (APP), and the accumulation of resulting amyloid β peptides (Aβ) in amyloid plaques is one of the earliest events occurring in Alzheimer's disease (AD), whereas the subsequent pathological pathways activated in the brain are still a topic of debate. This amyloid cascade hypothesis postulates that the formation of these plaques would enhance microglial and astrocytic activation and alter neuronal ionic homeostasis as well as oxidative injury. The consecutive alteration of the kinase and phosphatase activities ultimately would result in the formation of neurofibrillary tangles composed of hyperphosphorylated tau proteins. Finally, the widespread neuronal and synaptic dysfunctions generate the clinically observed cognitive symptoms including progressive memory loss, instrumental dysfunctions, and behavioural abnormalities [1]. Based on these assumptions, various transgenic mouse models for AD have been developed that over-express mutant forms of APP in an effort to elucidate the potential role of Aβ in the pathogenesis of the disease. The first model described in 1996 over-expressed the Swedish mutation of human APP and was called Tg2576 [2]. These mice exhibit elevated Aβ, as well as classic senile plaques with dense amyloid cores diffusely deposited in the neocortex and limbic areas. They are accompanied by changes in cholinergic neurotransmission that may underlie deficits in learning and memory observed at 8 months of age [3]. The amyloid plaques in these mice are associated with dystrophic neuritis and activated microglia [4]. All these studies demonstrated that Tg2576 was a

Abbreviations: Aβ, amyloid β; APP, Amyloid Precursor Protein; AD, Alzheimer's disease; ApoE, Apolipoprotein E; CSF, cerebrospinal fluid; DRP-2, dihydropyrimidinase-related protein-2; 2DE, two-dimensional electrophoresis; MS, mass spectrometry; MS/MS, tandem mass spectrometry; PMF, peptide mass fingerprint; SDS, sodium dodecyl sulfate

☆ This paper was presented at the Swiss Proteomics Society 2005 Congress, Zürich, Switzerland, 5–7 December 2005.

* Correspondence to: Neuroproteomics Group, Université de Genève, Centre Médical Universitaire, 1 rue Michel Servet, 1211 Geneva CH4, Switzerland. Tel.: +41 22 379 51 95; fax: +41 22 379 59 84.
E-mail address: Odile.Carrette@medecine.unige.ch (O. Carrette).

1570-0232/$ – see front matter © 2006 Elsevier B.V. All rights reserved.
doi:10.1016/j.jchromb.2006.05.019

relevant model to study, thus validating, the amyloid hypothesis. However, other studies have revealed that Tg2576 mice show a lower degree of inflammation and neurodegeneration than AD patients [5]. Double transgenic mice, called Tg2576PSEN1, carrying the same mutation on APP and a mutation on the gene coding for presenilin 1 are also useful for studying the Aβ deposition mechanism since amyloid plaques appear in the brain as early as 3–5 months of age in these mice [6].

Apolipoprotein E (ApoE) also appears to play a major role in the pathogenesis of AD, as the relative risk of developing dementia increases in individuals who inherit an ApoE ε4 allele. Individuals carrying the ApoE ε4 and developing AD, have a greater number of amyloid plaques. However, the precise role of ApoE in the pathogenesis of AD is still poorly understood. Several studies have shown that the mechanisms through which ApoE contributes to pathogenesis of AD include deposition, aggregation, and clearance of Aβ peptides [7,8]. More recently, an hypothesis under investigation by several groups supported that ApoE is involved in deposition and clearance of Aβ by direct protein–protein interaction [9,10]. Several studies already demonstrated that peptide fragments derived from ApoE are present in brain tissue of AD patients [7,11–13]. Immunohistological studies suggested that both C-terminal and N-terminal truncated forms of ApoE are associated with amyloid plaques [14] and neurofibrillary tangles in human AD brains [15]. Indeed, ApoE also plays a role in stabilizing neurofibrillary tangles [16] and in the disruption of cytoskeletal structure and function [17]. Employing a knockout strategy, the Tg2576 mice were crossed with ApoE null mice and showed a reduction of Aβ deposition, absence of neuritic degeneration, and reduction of vascular amyloidosis [18]. These authors concluded that ApoE affects the amount, morphology, and localization of Aβ deposits in Tg2576 mice. Whether endogenous murine ApoE in these APP mutant mice was undergoing truncation as in human AD brains was not demonstrated.

Proteomics is the strategy of choice to screen for simultaneous changes occurring in biochemical pathways during the course of AD. Such changes can occur as expression differences, post-translational modifications or proteolytic degradation that can be observed in two-dimensional electrophoresis (2DE). Changes in the proteome of the cortex have been reported by one group using Tg2576 at 24 months compared to control littermates [19]. Several proteins related to the neurodegenerative process were identified. However, authors of this study did not describe early changes occurring before detectable amyloid deposition. This issue is addressed in the present study.

Changes of the proteome were screened in the cortex of two transgenic mouse models (Tg2576 and Tg2576PSEN1) at 3 month and 2-year-old when the amyloid plaque load was absent and cover between 2% and 5.2% of the total cortex area, respectively. A variety of comparisons were made between the different mice used in this study to identify proteins changes with the highest biological significance. The results presented here demonstrate that a number of proteins were differentially expressed in APP transgenic mice even before the apparition of noticeable amyloid deposits. Additionally, in aged transgenic mice, the apparition of amyloid plaques was accompanied by an accumulation of murine ApoE fragments in the cortex. This study provided a basis for future experiments to determine the mechanisms by which the differentially expressed proteins are modulated in aging and plaque formation.

2. Experimental

2.1. Animals and tissues

Tg2576 mice expressing $APP_{K670N/M671L}$ at high level under control of the hamster prion protein (PrP) promoter have been described previously [2] (commercially available at Taconic Inc., Germantown, NY, USA). The double transgenic Tg2576PSEN1 mouse line was first developed by Jankowsky et al. [6]. The latter carries a mutation on the human presenilin 1 gene (commercially available at The Jackson Laboratory, Bar Harbor, ME, USA). These mice have an increased proportion of the Aβ42 peptide present in plaques with an accelerated deposition at 3–5 months. All animal studies were approved by the local ethical review committee, and were carried out in accordance with Swiss government regulations and NIH guidelines on the care and welfare of laboratory animals. This study included five different animal models: 3-month-old Tg2576 mice ($n = 2$), 3-month-old control littermates ($n = 2$), 2-year-old Tg2576 mice ($n = 2$) and Tg2576PSEN1 ($n = 1$), and 2-year-old control littermates ($n = 2$). Mice were anaesthetised with pentobarbital and perfused transcardially with 0.9% saline. Brains were removed, left cortex samples were snap frozen, lyophilized and kept at −80 °C for proteomic analysis.

2.2. Gel electrophoresis

All reagents and apparatus have been described previously [20]. All the gels were run in the same experiment. One hundred micrograms of lyophilized cortex tissue was suspended in 30 μl of Laemmli buffer [21] and loaded on to a 1DE pre-cast bis tris glycine gel NuPage 12% (Invitrogen, Basel, Switzerland). Gels were run under constant voltage (200 V) until the bromophenol blue front reached the end of the gel. For large 2DE analytical gels, 1 mg of lyophilized cortex was suspended in 400 μl of the rehydration buffer, i.e. 5 M urea, 2 M thiourea, 4% (w/v) CHAPS, 65 mM DTE, 2% (v/v) ampholines 4–8, and a trace of bromophenol blue. The samples were vortexed for 1 h at room temperature before rehydration of the non linear 18 cm IPG strips (GE Healthcare). Electrophoretic migration was performed as described previously [22]. Gels were silver stained [23]. A preparative 2DE gel was run with 2 mg of pooled lyophilized cortex from young and old mice. This gel was stained with Coomassie blue R250, and used for mass spectrometric analysis.

2.3. Protein visualization and software analysis

Stained gels were scanned with a laser densitometer. Scanned images were analyzed with ImageMaster™ 2D Platinum software powered by Melanie 4.0 (GE Healthcare and Genebio, Switzerland). Spots were detected and quantified automatically. The relative optical density (OD) and relative volume were com-

puted to correct for differences in gel staining. These measures take into account variations due to protein loading and staining, by considering the total OD or volume over all the spots in the gel. The digitized 2DE images of cortex were then compared by the matching method as described in the statistical analysis.

2.4. Protein Identification by tandem mass spectrometry

Spots of interest were cut out from the preparative 2DE gel and destained by washing twice with 30% acetonitrile in 50 mM ammonium bicarbonate for 45 min at 37 °C. Gel pieces were then dried for 30 min in a Hetovac vacuum centrifuge (HETO, Allerod, Germany). Dried pieces of gel were subjected to protein digestion by trypsin and peptide extraction using previous published protocols [24]. MS and MS/MS analysis of peptides from 2DE gel spots were performed with a 4700 Proteomics Analyzer MALDI-TOF/TOF mass spectrometer (Applied Biosystems, Framingham, MA, USA) according to the tuning procedures suggested by the manufacturer. Peak lists were generated with the Launch peak to Mascot tools with the following settings: for the MS data, mass range 850–4000, peak density of maximum 50 peaks per 200 Da, minimal signal to noise ratio of 10, minimal area of 100, max peak 200; for the MSMS data, mass range between 60 and 2000; peak density of maximum 50 peaks per 200 Da, minimal signal to noise ratio of 5, minimal area of 20, and maximum number of peak set at 200. Acquired MS and MS/MS data were compared to the database using the MASCOT search engine (http://www.matrixscience.com). The combined PMF and MS/MS search was performed on all entries present in UniProtSPTR database, version number 062005 containing 1929823 sequence entries at the time of the study. Search settings allowed two missed cleavages with the trypsin enzyme selected, three variable modifications (carboxymethylated cysteine, deamidation and oxidation of methionine), a peptide m/z tolerance of ±0.2 Da. A parent MS filtering was applied to the raw data between 800 Da and 4000 Da with a minimum S/N filter of 10. The MS/MS peak filtering was set between 60 Da and 20 Da below each precursor mass with a minimum S/N filter of 5.

2.5. Western blot

Proteins separated by 2DE or SDS–PAGE were electroblotted onto PVDF membranes as described by Towbin et al. [25]. Proteins of interest were detected using anti-human ApoE polyclonal antibodies (1:1000, Chemicon Int.) and an ECL™ western blotting detection kit (GE Healthcare). For stripping, the PVDF membranes were incubated for 30 min at 50 °C in a 62 mM Tris buffer containing 2% (w/v) SDS, 3% (w/v) DTE, pH 6.7. After rinsing with water, the stripped membranes were developed with the ECL™ kit again to check the absence of any immunoreactivity before probing with the anti-actin antibody (D1/200, Sigma–Aldrich).

2.6. Statistical analysis

The experimental gel containing the highest number of spots was selected as the reference gel. A linear regression analysis of all gels versus the reference gel was performed to evaluate the inter-gel variations of the vol% and to select a threshold value indicative of variability. A ratio of the means at 1.4 was applied to extract variable spots between different classes. Then spots variability as a function of transgene insertion, aging or amyloid plaque deposition was investigated. Two types of tests (with null hypothesis of no differential expression) at a 5% level risk were performed: a non parametric Wilcoxon Rank Sum test (Mann–Whitney), which does not make strong assumptions over the underlying distribution of the data and a Student test of differences in means. To perform the Student test on differences of means, the underlying assumptions on this test were checked. Namely, a Student t-test will provide valid and interpretable results if the underlying distribution of each sample is normally distributed and if the variances of each sample

Table 1
Results of the linear regression of the gels

Gel 1 vs. gel 2	a	b	$1/a$	$(a-1)\times 100\%$	R^2	Number of spots matched
5083[a] vs. Ref	0.5	0.04	2	−50	0.72	866
5084[a] vs. Ref	0.55	0.03	1.8	−45	0.72	869
5085[b] vs. Ref	0.65	0.01	1.54	−35	0.75	948
5086[c] vs. Ref	0.8	0.02	1.25	−20	0.8	796
5087[c] vs. Ref	0.57	0.05	1.75	−43	0.6	793
5089[d] vs. Ref	0.59	0.033	1.69	−41	0.56	847
5090[e] vs. Ref	0.64	0.065	1.56	−36	0.45	667
5091[e] vs. Ref	0.64	0.02	1.56	−36	0.78	935
5083[a] vs. 5084[a]	1.2	−0.018	0.83	20	0.848	1010
5087[c] vs. 5086[c]	1.3	−0.032	0.77	30	0.838	873
5090[e] vs. 5091[e]	1.4	0.015	0.71	40	0.713	637

The R^2 value indicates the quality of the fit. The inter-gel global scale variability in vol% is read as $(a-1)\times 100\%$, whereas b reads as offset variability. The number of spots matched is indicated in the last column.

[a] 2-year-old non transgenic.
[b] 2-year-old mice Tg2576PS1.
[c] 2-year-old mice Tg2576.
[d] 3-month-old non transgenic.
[e] 3-month-old Tg2576.

are equal. Given the small number of data, these assumptions were tested by applying the Shapiro-Wilks normality test and the Fisher equality of variance test. When the equality of variance was confirmed, a version of the Student comparison of two means test incorporating the Welsch/Satterthwaite correction was used. The issue of relative power of each test plays a role in the results.

3. Results

3.1. Two-dimensional gel electrophoresis statistical analysis

The representative gel used as the reference for the matching is shown in Fig. 1 and linear regression of all the gels are given in Table 1. The values of the R^2 coefficients indicate a good fit in general on the matched gels and perfectly tolerable variations in the scale of the vol% measures. For each gel, they vary between −50% and −20% on average with respect to the reference gel. The significance of the linear regression coefficient should be acceptable given the high number of spots matched between the reference gel and other gels. A linear regression was also computed for gel belonging to the same class. The regression shows a very acceptable level overall homogeneity in the vol% expression between the two 'designed-as-homogenous' gels (maximum 40% variability). Therefore, a threshold for the ratio of the means was set at 1.4 as indicative of a variation between two classes. Using such criteria, we performed a differential analysis with Image Master depending on three different variables: the effect of transgene addition, the age effect, and the consequences of the amyloid plaque deposition. Ten spots showing a variation upon one of these effects were selected for fine statistical analysis as described in Section 2 and reported in Table 2. The linear regression analysis across all class for these 10 spots confirmed a maximal intra-class variability of 40%.

In order to identify protein varying upon the APP transgene addition, the Tg2576 mice ($n = 4$), aged of 3 and 24 months, were compared to the controls ($n = 4$), young and old. Both Stu-

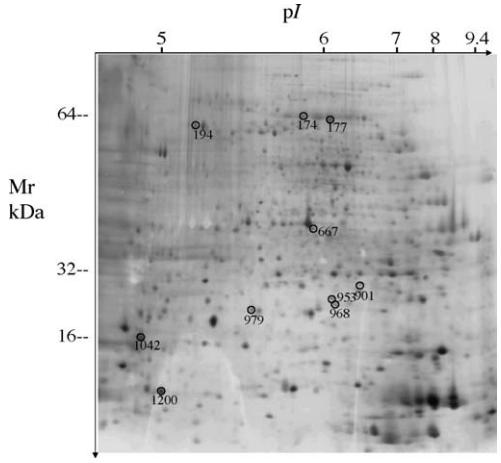

Fig. 1. Gel image of silver-stained 2DE showing protein spots identified by MALDI-TOF-TOF. First dimension was performed on pH 3.5–10 IPG strips. Second dimension was run on home-made acrylamide gradient 9–16% T gels.

Table 2
Identified differentially expressed protein spots

Spot	Protein identified	SwissProt accession number	Transgene effect					AGE effect					Amyloid deposit effect				
			Change	No Tg ($n = 4$) mean ± SD	Tg2576 ($n = 4$) mean ± SD	*T*-test *p*-value	Wilcoxon *p*-value	Change	Young ($n = 4$) mean ± SD	Old ($n = 5$) mean ± SD	*T*-test *p*-value	Wilcoxon *p*-value	Change	No Plaque ($n = 6$) mean ± SD	Plaque ($n = 3$) mean ± SD	*T*-test *p*-value	Wilcoxon *p*-value
1042	Alpha-synuclein	O55042	Up	0.395 ± 0.043	0.776 ± 0.079	0.0003	0.0142	ns	0.656 ± 0.203	0.534 ± 0.268	0.424	0.365	ns	0.507 ± 0.182	0.629 ± 0.33	0.299	0.357
1200	Cytochrome oxidase polypeptide Va	P12787	Up	0.267 ± 0.083	0.552 ± 0.023	0.0022[a]	0.0142	ns	0.445 ± 0.138	0.349 ± 0.182	0.199[b,a]	0.206	ns	0.364 ± 0.164	0.446 ± 0.176	0.270[b,a]	0.273
667	Alpha enolase	P17182	ns	0.075 ± 0.018	0.085 ± 0.025	0.229	0.442	Up	0.066 ± 0.01	0.092 ± 0.023	0.035	0.0158	ns	0.074 ± 0.014	0.094 ± 0.031	0.190	0.190
979	UMP-CMP kinase	Q9DBP5	ns	0.051 ± 0.029	0.063 ± 0.024	0.273	0.242	Down	0.079 ± 0.011	0.032 ± 0.009	0.0003	0.008	Down	0.062 ± 0.028	0.036 ± 0.01	0.046	0.190
968	ATP synthase α chain	Q03265	ns	0.068 ± 0.021	0.079 ± 0.015	0.125	0.242	Up	0.061 ± 0.009	0.085 ± 0.016	0.0159	0.031	Up	0.067 ± 0.016	0.088 ± 0.013	0.047	0.047
953	ATP synthase α chain	Q03265	ns	0.060 ± 0.017	0.073 ± 0.014	0.125	0.1	Up	0.051 ± 0.010	0.078 ± 0.013	0.0146	0.031	Up	0.058 ± 0.013	0.082 ± 0.015	0.076	0.047
901	ATP synthase α chain	Q03265	ns	0.057 ± 0.010	0.066 ± 0.020	0.239	0.342	Up	0.050 ± 0.005	0.071 ± 0.017	0.0326[a]	0.031	Up	0.052 ± 0.009	0.078 ± 0.018	0.074	0.023
174	Dihydropyrimidinase-related protein-2	O08553	ns	0.208 ± 0.027	0.217 ± 0.163	0.348[a]	0.557	Down	0.293 ± 0.132	0.149 ± 0.054	0.057	0.031	Down	0.264 ± 0.112	0.111 ± 0.009	0.010[b,a]	0.011
177	Dihydropyrimidinase-related protein-2	O08553	ns	0.258 ± 0.053	0.218 ± 0.102	0.414	0.557	ns	0.279 ± 0.07	0.201 ± 0.079	0.0844	0.142	Down	0.273 ± 0.066	0.162 ± 0.061	0.031	0.083
194	ATP synthase β chain	P56480	ns	0.144 ± 0.052	0.121 ± 0.083	0.467	0.657	ns	0.158 ± 0.059	0.109 ± 0.072	0.148	0.142	Down	0.161 ± 0.056	0.071 ± 0.049	0.031[b,a]	0.047

Mean values are expressed in vol%.
[a] Indicates a rejection of the equality of variance, a *T*-test with correction for inequality of variances is used. Given the potentially low power of all the tests we use, the *p*-values of a Wilcoxon Rank Sum test over the means is also given.
[b] Indicates a rejection of the normality distribution. *T*-test is not applicable.

Table 3
MALDI-TOFTOF identification

Spot number	Protein identified	SwissProt accession number	Exp[a] p*I*	Theo[a] p*I*	Exp[a] Mr	Theo[a] Mr	PMF peak match %coverage[b]	Peptide identified by MSMS	Peptide ion score (Mascot threshold)
1042	Alpha-synuclein	O55042	4.7	4.74	14000	14476	54	TVEGAGNIAAATGFVK EQVTNVGGAVVTGVTAVAQK TKEQVTNVGGAVVTGVTAVAQK TVEGAGNIAAATGFVKK TKEGVVHGVTTVAEK TKEGVLYVGSK	123 (threshold 45) 56 51 37 22 19
1200	Cytochrome oxidase polypeptide Va	P12787	5.0	5.01	10000	12436	37	SHGKQETDEEFDA RLNDFASAVR	47 (threshold 46) 31
667	Alpha enolase	P17182	5.95	6.36	47000	47009	34	SGKYDLDFKSPDDPSR AGYTDQVVIGMDVAASEFYR YITPDQLADLYK YNQILRIEEELGSK AGAVEKGVPLYR SFRNPLAK	32 (threshold 48) 34 24 23 20 11
901	ATP synthase alpha chain	Q03265	6.4	8.28	28000	55310	23	EAYPGDVFYLHSR EVAAFAQFGSDLDAATQQLLSR QGQYSPMAIEEQVAVIYAGVR	82 (threshold 49) 40 17
968	ATP synthase alpha chain	Q03265	6.0	8.28	21000	55310	24	EVAAFAQFGSDLDAATQQLLSR LKEIVTNFLAGFEP QGQYSPMAIEEQVAVIYAGVR	72 (threshold 49) 47 20
953	ATP synthase alpha chain	Q03265	6.0	8.28	22000	55310	28	EVAAFAQFGSDLDAATQQLLSR LKEIVTNFLAGFEP	64 (threshold 48) 64
194	ATP synthase beta chain	P56480	5.1	4.99	60000	51749	58	AHGGYSVFAGVGER VLDSGAPIKIPVGPETLGR AIAELGIYPAVDPLDSTSR IMDPNIVGNEHYDVAR LVLEVAQHLGESTVR VALVYGQMNEPPGAR VVDLLAPYAK	125 (threshold 48) 83 68 55 40 31 17
979	UMP-CMP kinase	Q9DBP5	5.6	5.68	21000	22165	65	NKFLIDGFPR TMDGKADVSFVLFFDCNNEICIER	32 (threshold 45) 2
174	Dihydropyrimidinase-related protein-2	O08553	5.9	5.95	62000	62170	47	KPFPDFVYKR AVGKDNFTLIPEGTNGTEER IVLEDGTLHVTEGSGR NLHQSGFSLSGAQIDDNIPRR DIGAIAQVHAENGDIIAEEQQR	56 (threshold 48) 29 25 20 15
177	Dihydropyrimidinase-related protein-2	O08553	5.8	5.95	62000	62170	41	KPFPDFVYKR AVGKDNFTLIPEGTNGTEER GLYDGPVCEVSVTPK	26 (threshold 51) 6 20

[a] Exp and Theo stands for Experimental and Theoretical, respectively.
[b] PMF peak match is generated by MASCOT and represented as the %coverage of the mature protein sequence described in the database.

dent *t*-test and Wilcoxon test showed that two spots differed significantly between the transgenic and the control group suggesting that these proteins expression was dependant on genotype (Table 2). They were identified as the α-synuclein and the cytochrome oxidase polypeptide Va.

The effect of aging was estimated by comparing all the 2-year-old mice ($n=5$), control, Tg2576 and Tg2576PSEN1, to the 3-month-old mice, control and Tg2576 ($n=4$). Six spots were found differential at the 5% level, four spots increased upon aging among which α enolase, and three isoforms of ATP synthase α chain; while two spots decreased including UMP-CMP kinase, dihydropyrimidinase-related protein-2 (DRP-2).

Changes upon amyloid deposition were investigated in three transgenic mice of 2-year-old (Tg2576, $n=2$, and Tg2576PSEN1, $n=1$) versus all the other mice where no significant amyloid deposition was observed by microscopy. Histological examination confirmed the deposition of amyloid into plaques. Their surface area represented 2.05 % of the cortex in 2-year-old Tg2576 and up to 5.3% in aged Tg2576PSEN1 (data not shown). The three isoforms of ATP synthase α chain were found up-regulated with the Wilcoxon test. While, UMP-CMP kinase, two isoforms of DRP-2 and ATP synthase β chain were found significantly down-regulated.

Table 3 summarizes both PMF data and peptide sequenced by MS/MS for these 10 spots that were considered to validate the identification using MASCOT search engine to interrogate the UniProtSPTR database.

3.2. Western blot analysis of Apolipoprotein E

Several studies support the hypothesis that ApoE participates in an age-related abnormal regulation of Aβ clearance and amyloid deposition. To further validate this assumption, the expression of murine ApoE was assessed by western blot

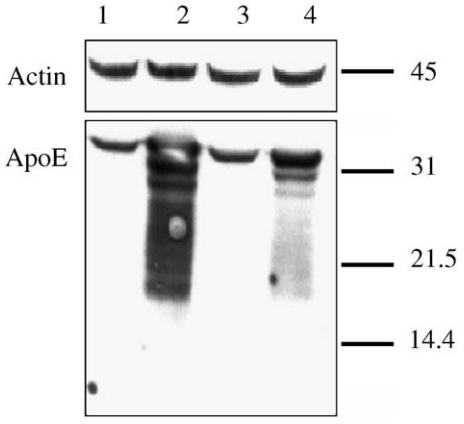

Fig. 2. Western blot analysis of ApoE immunoreactivity after separation by SDS–PAGE. One hundred micrograms of cortex samples were run on a 12% bis tris polyacrylamide gel (Novex). Following transfer to PVDF, ApoE isoforms and fragments were detected with anti-human ApoE polyclonal antibody (1:1000, Chemicon Int.) and developed by ECL. Then the blot was stripped and reprobed with anti-actin antibody (1:200, Sigma–Aldrich). Lane 1, 3-month-old Tg2576 mouse; lane 2, 2-year-old Tg2576PSEN1 mouse; lane 3, 3-month-old control littermate of the Tg2576 mouse line; lane 4, 2-year-old Tg2576 mouse.

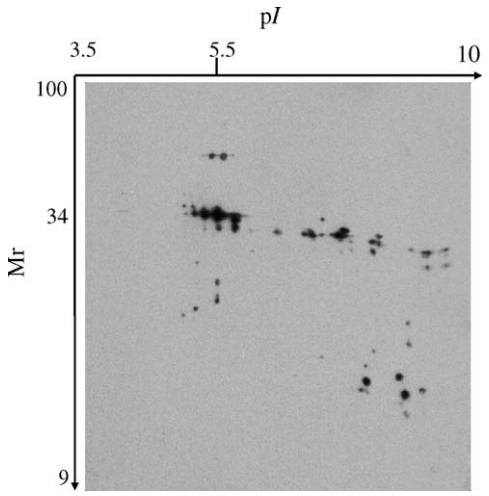

Fig. 3. Western blot analysis of ApoE immunoreactivity after separation by large format 2DE. One milligram of cortex sample of a 2-year-old double transgenic mouse (Tg2576PSEN1) was resolved on a large 2DE gel. Following transfer to PVDF, ApoE isoforms and fragments were detected with anti-human ApoE polyclonal antibody (1:1000, Chemicon Int.) and developed by ECL.

images. SDS–PAGE revealed that ApoE was over-expressed in both single and double transgenic old mice and that many ApoE fragments were produced in the cortex of both type of mice when compared to the young mice (Fig. 2). However, ApoE over-expression was of greater magnitude in Tg2576PSEN1 than in Tg2576 mice, while the actin band was equivalent in all the samples loaded onto the gel. A cortex sample from the 2-year-old Tg2576PSEN1 was separated by 2DE gel and electroblotted on to a PVDF membrane for probing with anti-ApoE antibodies (Fig. 3). As expected from the SDS–PAGE results, many ApoE isoforms and fragments were present in the cortex of this mouse. The main reactivity was found at the expected Mr and p*I* of the full length ApoE (34 kDa and 5.5, respectively). A number of truncated fragments of Mr below 34 kDa were recognized as well. Some of these fragments have a very basic p*I* compared to the full length ApoE. A faint reactivity was observed at a Mr higher than 34 kDa. These two spots could correspond to aggregated ApoE.

4. Discussion

The Tg2576 mice contain mutant forms of APP that drive the production of Aβ40 and Aβ42, and the deposition of amyloid plaques in the brain. They recapitulate the amyloid-related neuropathology characteristic of AD patients [2], despite the fact that these mice do not show as much neurofibrillary pathology as observed in humans. Numerous studies using these transgenic mice have been undertaken to understand the degeneration pathways induced by APP and amyloid peptides. Proteomics is an ideal technology for detecting changes in protein expression occurring in the process of development and aging of genetically engineered mice. The present study demonstrated that specific changes in the proteome occur in the cortex of transgenic mouse models for AD upon transgene expression, aging and amyloid plaque deposition.

4.1. Age-independent molecular changes that were specifically related to mutant APP expression

Compensatory and adaptive mechanisms are likely to occur upon a transgene expression in animal models. Using similar models to those of our study, Skynner et al. [26] have found between 4 and 8 protein spots consistently differentially expressed between genetically altered and wild-type mice. They could identify an isoform change of mortalin in the Tg2576 mice. In our study, we identified two proteins that increased upon transgene addition: α-synuclein and cytochrome oxidase polypeptide Va. Alpha-synuclein, also known as the non-Aβ component of AD amyloid, is a pre-synaptic terminal molecule that accumulates in the plaques and amyloid-enriched fractions from AD brain [27]. Our results show that up-regulation of APP is associated to an up-regulation of α-synuclein at 3 months, even before the apparition of amyloid deposits. This could explain why in aged Tg2576 mice, α-synuclein was found to be a major intracellular accumulating protein in neurites resembling those seen in the Lewy body variant of AD [28]. The co-regulation pathways of the expression of these genes remain to be clarified.

4.2. Ageing molecular changes and Amyloid plaque deposition effect in transgenic APP mice

One of the difficulties encountered when studying such age-related phenotypes is to distinguish between age-dependent and age-independent molecular changes. To address this issue we compared the proteome map of all aged animals to the 3-month-old animals included in this study, and then differentiate them from the plaque bearing animals.

In humans, ageing remains the most important but poorly understood risk factor for dementia and especially AD. Ageing can be considered as a progressive, inevitable process partly related to the oxidative damage of biomolecules that is not counteracted by protective functions. Disruptions in energy metabolism have been suggested to be a prominent feature. Because mitochondria are the major site of free radical production in cells, they are also a primary target for oxidative damage and subsequent dysfunction. The main protein changes found in our study related to aging were associated to the energy metabolism and mitochondrial enzymes. Indeed, we found three different spots identified as ATP synthase α chain up-regulated in the aged mice and in presence of amyloid deposits. Interestingly, a cytosolic accumulation of ATP synthase α chain has been documented in neurofibrillary degeneration of AD [29]. Therefore, our results are further validating the Tg2576 model as a relevant model to study AD neurodegeneration processes. Since ATP, the energy source is generated through glycolysis, it is not surprising to observe a concomitant increase of α-enolase that catalyses 2-phospho-D-glycerate in phosphoenol-pyruvate. Up-regulation of α-enolase might be a compensatory mechanism for the increased activity of the ATP synthase in aging. Increase of murine brain α-enolase upon aging has also been reported previously by others [30]. Previous work suggested that protein levels of glycolytic enzymes might be up-regulated during aging to compensate for the metabolic decline of mitochondrial respiration. Alpha-enolase may be part of that glycolytic compensation.

In our study, we found a down-regulation of dihydropyrimidinase-related protein-2 (DRP-2) upon aging. This result was in contradiction to the up-regulation of DRP-2 in old mice brain observed by Poon et al. [30]. However, such a dys-regulation and high heterogeneity was confirmed by Lubec et al. studying the expression at the mRNA and protein levels of DRP-2 in down syndrome and AD brains [31]. A decrease of DRP-2 was also found in a 2DE gel study on AD brains, however the same authors found increased of ATP synthase β chain, decrease of ATP synthase α chain and apparently no change on α-synuclein [32]. Finally, a comparative study of 2-year-old Tg2576 mice versus old control littermates was performed by Shin et al. [19]. Several proteins identified in their study were also found differentially expressed in ours, although some of the changes that we observed were in the opposite direction. These authors observed an increase of the α-enolase as we did; and, they did not see any difference in the α-synuclein protein, the ATP synthase α chain was down-regulated and the DPR-2 was up-regulated. ATP synthase α chain and DRP-2 are represented in 2DE as several spots. The differences observed between the different studies could be associated with different specific isoforms. The actual variations of their expression should be studied on a time course basis and with an absolute quantitative technology such as an ELISA assay.

In summary, the proteins identified in this study are undoubtedly dys-regulated in the pathologic processes associated with aging and/or amyloid deposition in the brain. The pathways regulating the expression of these energy metabolisms-related proteins must be further elucidated to potentially propose them as targets for compensatory therapy in AD.

4.3. Murine Apolipoprotein E is truncated in old transgenic mice

In humans, colocalisation of ApoE and Aβ in senile plaques has been proved by immunohistochemical studies and revealed the presence of ApoE fragments when specific antibodies directed against N-terminal and C-terminal part of the protein were used [14]. The evidence of the neurotoxicity of human ApoE fragments has also been shown in vitro [33] and reviewed in detail elsewhere [34]. Considering the numerous studies using APP mouse models, the lack of information concerning the murine ApoE and potential variants similar to the human variants is surprising. Interestingly, human ApoE and mouse ApoE exhibit 72% identity. Moreover, the mouse ApoE as described in the SwissProt database carries two Arg residues resembling those in the human ApoE ε4 isoform. Therefore, we can hypothesize that changes in endogenous murine ApoE occurring in these transgenic mice models could reflect what is happening in human upon senile plaque deposition. Kuo et al. [35] measured murine ApoE levels in brains of Tg2576 mice and controls at intervals between 2 and 20 months by scanning densitometry of western blot. These authors suggested that the amount of endogenous ApoE in the brains of Tg2576 mice compared to control littermates was elevated by an average of 45% at 2

months; and up to 60% at the age of 20 months. However, no western blot image was provided in that paper and surprisingly the authors did not report the presence of ApoE fragments. In our study, we investigated the behaviour of endogenous murine ApoE by western blot images. We demonstrated that murine ApoE is cleaved in aged transgenic mice and this truncation seemed enhanced by the accumulation of amyloid deposits. Murine microglial cells have been found to produce truncated ApoE in vitro [36], which may correspond to the ApoE fragments observed in the present study. The higher molecular weight spots highlighted by the antibody used in our study may correspond to the aggregation of ApoE, which has also recently been described in human AD [37].

The protease responsible for the cleavage of ApoE could potentially be a therapeutic target for prevention and treatment of AD. Research aimed at identifying this protease is therefore a high priority. In vitro experiments have shown that a wide range of proteases can cleave ApoE, yielding N- and C-terminal fragments [38]. However, no specific protease responsible for ApoE cleavage in vivo has yet been identified. Surprisingly, no previous study has shown the ApoE fragments by 2DE and no literature concerning the p*I* of these fragments has been found that would help to unravel the type of cleavage. Our results suggest that the APP mouse models might be highly valuable to screen for ApoE proteases and corresponding inhibitors. Whether cleavages of ApoE occur before or after deposition in the amyloid plaques also remain to be clarified and could be investigated in these mouse models.

4.4. Concluding remarks

In conclusion, the present study demonstrated specific AD-associated protein changes in the cortex of APP transgenic mouse models. These changes appear to be related to three distinct processes that are likely to intermingle in the pathogenesis of AD, including a particular genetic background, an effect of age and the burden of amyloid deposition. Altered protein expression is reflected notably in quantitative changes of protein level in comparative samples, but also in more subtle qualitative modifications, as exemplified by the truncation of murine ApoE found here.

Acknowledgements

The authors would like to thank Bayer AG, Wuppertal Germany, for generously providing the mouse brain samples used in this study. Animals were housed in their facility and they hold ethical authorization for performing the study. Additionally, we received ethical approval according to the Swiss government regulations for performing the particular research project as stated in Section 2.

References

[1] J. Hardy, D.J. Selkoe, Science 297 (2002) 353.
[2] K. Hsiao, P. Chapman, S. Nilsen, C. Eckman, Y. Harigaya, S. Younkin, F. Yang, G. Cole, Science 274 (1996) 99.
[3] J. Apelt, A. Kumar, R. Schliebs, Brain Res. 953 (2002) 17.
[4] A. Sasaki, M. Shoji, Y. Harigaya, T. Kawarabayashi, M. Ikeda, M. Naito, E. Matsubara, K. Abe, Y. Nakazato, Virchows Arch. 441 (2002) 358.
[5] G. Munch, J. Apelt, E. Rosemarie Kientsch, P. Stahl, H.J. Luth, R. Schliebs, J. Neurochem. 86 (2003) 283.
[6] J.L. Jankowsky, H.H. Slunt, T. Ratovitski, N.A. Jenkins, N.G. Copeland, D.R. Borchelt, Biomol. Eng. 17 (2001) 157.
[7] T. Wisniewski, M. Lalowski, A. Golabek, T. Vogel, B. Frangione, Lancet 345 (1995) 956.
[8] C.A. Lemere, J.K. Blusztajn, H. Yamaguchi, T. Wisniewski, T.C. Saido, D.J. Selkoe, Neurobiol. Dis. 3 (1996) 16.
[9] D.R. Thal, E. Capetillo-Zarate, C. Schultz, U. Rub, T.C. Saido, H. Yamaguchi, C. Haass, W.S. Griffin, K. Del Tredici, H. Braak, E. Ghebremedhin, Acta Neuropathol. (Berl.) (2005).
[10] D.B. Carter, Subcell. Biochem. 38 (2005) 255.
[11] M.A. Marques, M. Tolar, J.A. Harmony, K.A. Crutcher, Neuroreport 7 (1996) 2529.
[12] Y. Huang, X.Q. Liu, T. Wyss-Coray, W.J. Brecht, D.A. Sanan, R.W. Mahley, Proc. Natl. Acad. Sci. U.S.A. 98 (2001) 8838.
[13] F.M. Harris, W.J. Brecht, Q. Xu, I. Tesseur, L. Kekonius, T. Wyss-Coray, J.D. Fish, E. Masliah, P.C. Hopkins, K. Scearce-Levie, K.H. Weisgraber, L. Mucke, R.W. Mahley, Y. Huang, Proc. Natl. Acad. Sci. U.S.A. 100 (2003) 10966.
[14] H.S. Cho, B.T. Hyman, S.M. Greenberg, G.W. Rebeck, J. Neuropathol. Exp. Neurol. 60 (2001) 342.
[15] Y. Aizawa, R. Fukatsu, Y. Takamaru, K. Tsuzuki, H. Chiba, K. Kobayashi, N. Fujii, N. Takahata, Brain Res. 768 (1997) 208.
[16] W.J. Strittmatter, A.M. Saunders, M. Goedert, K.H. Weisgraber, L.M. Dong, R. Jakes, D.Y. Huang, M. Pericak-Vance, D. Schmechel, A.D. Roses, Proc. Natl. Acad. Sci. U.S.A. 91 (1994) 11183.
[17] B.P. Nathan, K.C. Chang, S. Bellosta, E. Brisch, N. Ge, R.W. Mahley, R.E. Pitas, J. Biol. Chem. 270 (1995) 19791.
[18] M.C. Irizarry, G.W. Rebeck, B. Cheung, K. Bales, S.M. Paul, D. Holzman, B.T. Hyman, Ann. N. Y. Acad. Sci. 920 (2000) 171.
[19] S.J. Shin, S.-E. Lee, J.H. Boo, M. Kim, Y.-D. Yoon, S.-I. Kim, I. Mook-Jung, Proteomics 4 (2004).
[20] D.F. Hochstrasser, S. Frutiger, N. Paquet, A. Bairoch, F. Ravier, C. Pasquali, J.C. Sanchez, J.D. Tissot, B. Bjellqvist, R. Vargas, et al., Electrophoresis 13 (1992) 992.
[21] U.K. Laemmli, Nature 227 (1970) 680.
[22] J.M. Deshusses, J.A. Burgess, A. Scherl, Y. Wenger, N. Walter, V. Converset, S. Paesano, G.L. Corthals, D.F. Hochstrasser, J.C. Sanchez, Proteomics 3 (2003) 1418.
[23] B. Bjellqvist, C. Pasquali, F. Ravier, J.C. Sanchez, D. Hochstrasser, Electrophoresis 14 (1993) 1357.
[24] O. Carrette, I. Demalte, A. Scherl, O. Yalkinoglu, G. Corthals, P. Burkhard, D.F. Hochstrasser, J.C. Sanchez, Proteomics 3 (2003) 1486.
[25] H. Towbin, T. Staehelin, J. Gordon, Proc. Natl. Acad. Sci. U.S.A. 76 (1979) 4350.
[26] H.A. Skynner, T.W. Rosahl, M.R. Knowles, K. Salim, L. Reid, R. Cothliff, G. McAllister, P.C. Guest, Proteomics 2 (2002) 1018.
[27] A. Takeda, M. Hashimoto, M. Mallory, M. Sundsumo, L. Hansen, A. Sisk, E. Masliah, Lab. Invest. 78 (1998) 1169.
[28] F. Yang, K. Ueda, P. Chen, K.H. Ashe, G.M. Cole, Brain Res. 853 (2000) 381.
[29] N. Sergeant, A. Wattez, M. Galvan-valencia, A. Ghestem, J.P. David, J. Lemoine, P.E. Sautiere, J. Dachary, J.P. Mazat, J.C. Michalski, J. Velours, R. Mena-Lopez, A. Delacourte, Neuroscience 117 (2003) 293.
[30] H.F. Poon, R.A. Vaishnav, T.V. Getchell, M.L. Getchell, D.A. Butterfield, Neurobiol. Aging (2005).
[31] G. Lubec, M. Nonaka, K. Krapfenbauer, M. Gratzer, N. Cairns, M. Fountoulakis, J. Neural. Transm. Suppl. 57 (1999) 161.
[32] T. Tsuji, A. Shiozaki, R. Kohno, K. Yoshizato, S. Shimohama, Neurochem. Res. 27 (2002) 1245.
[33] M. Tolar, J.N. Keller, S. Chan, M.P. Mattson, M.A. Marques, K.A. Crutcher, J. Neurosci. 19 (1999) 7100.
[34] M.A. Marques, K.A. Crutcher, J. Mol. Neurosci. 20 (2003) 327.

[35] Y.M. Kuo, F. Crawford, M. Mullan, T.A. Kokjohn, M.R. Emmerling, R.O. Weller, A.E. Roher, Mol. Med. 6 (2000) 430.
[36] Q. Xu, Y. Li, C. Cyras, D.A. Sanan, B. Cordell, J. Biol. Chem. 275 (2000) 31770.
[37] D. Fan, Q. Li, L. Korando, W.G. Jerome, J. Wang, Biochemistry 43 (2004) 5055.
[38] J.R. Wetterau, L.P. Aggerbeck, S.C. Rall Jr., K.H. Weisgraber, J. Biol. Chem. 263 (1988) 6240.